Scale invariant spatio-temporal patterns of field vole density

JAMES L. MACKINNON*, STEVE J. PETTY¶, DAVID A. ELSTON†,
CHRIS J. THOMAS‡, TOM. N. SHERRATT§ and X. LAMBIN*

**Department of Zoology, University of Aberdeen, Tillydrone Avenue, Aberdeen AB24 2TZ; †Biomathematics
and Statistics Scotland, Environmental Modelling Unit, Macaulay Land Use Research Institute, Craigiebuckler,
Aberdeen AB15 8QH; ‡Department of Biological Sciences, University of Durham, South Road, Durham DH1 3LE;
and §Forest Research, Woodland Ecology Branch, Northern Research Station, Roslin, Midlothian EH25 9SY, UK*

Summary

1. Recent characterizations of the spatial scale of population dynamics have typically considered patterns at a single scale and ignored the possibility that different patterns may arise at different scales. In this study we assessed population densities of field voles with cyclic dynamics in northern England at 147 sites from three spatial scales on five occasions over a 2·5-year period.

2. The scale over which densities were similar was estimated by comparing the variance of density at the three scales (< 1 km^2, 10 km^2, and 70 km^2) and by using autocorrelation techniques. Closer sites were more similar in density than more distant sites and the autocorrelations suggested that sites up to within 8–20 km had more similar densities and higher population synchrony than the average similarity for all the sampling sites.

3. A generalized additive model fitted to all the data showed that the data supported the hypothesis of a travelling wave of vole densities moving through the study area. The model assumed that the wave moved at a constant speed and in a uniform direction. Estimates of the wave's speed (14 km year^{-1}) and direction (travelling in a direction of 66° from north) were consistent with the estimates which had previously been calculated from a time series of vole densities covering a much smaller spatial area but a longer temporal scale.

4. The spatio-temporal pattern of vole densities detected over a small spatial scale therefore appears to extend over much larger scales and occurs despite the fragmentation of suitable vole habitat at local (a few square kilometres) and regional (hundreds of square kilometres) scales.

Key-words: field voles, Kielder, *Microtus agrestis*, population synchrony, spatial scale, travelling wave.

Journal of Animal Ecology (2001) **70**, 101–111

Introduction

There is a new emphasis in population dynamics aimed at explaining spatial as well as temporal patterns in abundance (e.g. Legendre & Fortin 1989; Wiens 1989; Legendre 1993; Underwood & Chapman 1996; Bjørnstad 1997; Bjørnstad, Stenseth & Saitoh 1999a; Koenig 1999). Three factors are usually considered important in determining the patterns of synchrony for populations. They include climatic events (Moran 1953; Royama 1992; Grenfell *et al.* 1998), community processes and trophic interactions combined with dispersal (Ydenberg

1987; Ims & Steen 1990; Korpimäki 1994; Bjørnstad, Ims & Lambin 1999b; Sherratt *et al.* 2000) and delayed density dependence combined with dispersal (Ranta *et al.* 1995a; Steen, Ims & Sonerud 1996).

Identifying the possible causal mechanisms from observed spatial patterns in population synchrony is a challenge to population ecologists. One approach is based on the idea that different mechanisms lead to different 'scales of synchrony' or spatial domain over which populations lose their synchrony (e.g. Pollard 1991; Ranta *et al.* 1995a,b; Sutcliffe, Thomas & Moss 1996; Bjørnstad 1997; Myers, Mertz & Bridson 1997; Bjørnstad *et al.* 1999a; Paradis *et al.* 1999). A complementary approach has been to fit models with different dispersal functions to population growth models (Ranta *et al.* 1995a; Lele, Tapper & Gage 1998). Recently,

Correspondence: X. Lambin, Department of Zoology, University of Aberdeen, Tillydrone Avenue, Aberdeen AB24 2TZ, UK. E-mail: x.lambin@abdn.ac.uk Fax: + 44 (0)1224 2723796

Bjørnstad, Ims & Lambin (1999b) suggested that the spatial covariance function, which is the way the abundance or population growth rate depends statistically on neighbouring or more distant populations, could be used to identify the working of different processes. However, much theoretical work is still needed to generate robust predictions about the relationship between covariance functions and underlying processes, and little is known about the patterns expected when more than a single process shapes spatial synchrony simultaneously. In some instances, different processes are thought to operate simultaneously at local and regional scales. For example, Sutcliffe, Thomas & Moss (1996) suggested that climate synchronized populations of butterflies over distances up to 200 km whereas the dispersal ability of a species was a good predictor of its degree of synchrony at scales of 0·1–2 km (see also Paradis *et al*. 1999). Thus, a prerequisite to inferring processes responsible for a given pattern of synchrony is the characterization of patterns at a hierarchy of scales in order to determine whether they vary with sampling scale. This has rarely proved possible as few data sets have been collected for the purpose of characterizing patterns of synchrony, and patterns detected are constrained to an unknown degree by the extent and grain of the sampling regime (Wiens 1989).

Spatially explicit theoretical models have been used to provide some general insights on how dispersal, weather and trophic interaction may promote synchrony and how their influence depends on the underlying dynamics. These models show that when predators cover large areas, rapidly track their prey and have high impact on prey abundance, the synchrony of prey populations can occur over large spatial scales (Ims & Steen 1990; De Roos, McCauley & Wilson 1991). However, when close-coupled, specialized host–enemy or predator–prey interactions result in cyclic temporal dynamics, complex spatio-temporal patterns in the densities of both interacting species can arise (Kareiva 1990; Holmes *et al*. 1994; Gurney *et al*. 1998). Periodic travelling waves of density result from oscillatory predator–prey systems that incorporate random movement of the predator (Murray 1989; McCauley, Wilson & De Roos 1996; Sherratt, Eagan & Lewis 1997; Gurney *et al*. 1998). Predator–prey dynamics, however, is not the only ecological interaction leading to the formation of travelling waves; they have also been described in epidemiological models (Murray 1989), in models of populations structured by age (Holmes *et al*. 1994), in competition models (Cruywagen *et al*. 1996) and models of mutualistic relationships (Mischaikow & Hutson 1993).

Until recently, there was little evidence that complex patterns such as travelling waves in ecological systems were more than a mathematical curiosity. However, data suggestive of periodic travelling waves have recently been reported for densities of snowshoe hares (*Lepus americanus* Erxleben) in Canada (Smith 1983; Ranta, Kaitala & Lindström 1997) and microtine rodents in Fennoscandia (Fredga *et al*. 1993; Ranta &

Kaitala 1997). Lambin *et al*. (1998) used a generalized additive model to demonstrate that field vole (*Microtus agrestis* L.) densities varied as a travelling wave-like pattern within a commercial spruce forest in northern England and estimated that the wave moved approximately north-east at 19 km year^{-1}. Theoretically, the speed of travelling waves should relate to the diffusion rate of the process causing the wave, although it is also dependent on the details of the reaction process generating the fluctuations at any given location. Lambin *et al*. (1998) suggested that, although the average speed of the wave was 19 km year^{-1}, the speed varied and was highest in the late increase and late decrease stages of the population cycle. In that study all the sampling was conducted in one watershed of the forest (approximately 150 km^2), and it was therefore impossible to check whether the speed or direction of the wave differed in other parts of the forest. Hence, it was not clear whether the travelling wave detected at the scale of a single watershed was part of a large-scale pattern such as those suggested for *L. americanus* in Canada (Smith 1983) and field voles in Fennoscandia (Ranta & Kaitala 1997). Alternatively, any direction and speed detected for a wave at a large scale could be the average of several waves occurring at smaller scales with their direction resulting from the local variation in the permeability of the landscape to dispersal.

In this study we used the multiscale approach advocated by Wiens (1989) to document spatial patterns in densities of field vole, *M. agrestis* populations with cyclic temporal dynamics. We could estimate the effect of sampling scale on variation in vole densities because we sampled at three different spatial scales. This allowed us to relate the spatio-temporal pattern of vole densities detected in a 2·5-year period to the travelling wave pattern previously demonstrated by Lambin *et al*. (1998) using longer-term data in the same region but over a much smaller area. We show that the directional wave-like pattern previously detected at small scales is part of a larger pattern.

Materials and methods

STUDY SITE

We studied vole populations in a commercially managed conifer plantation in Northumberland, England (Fig. 1). The forest covers an area of approximately 600 km^2 and is dominated by spruces, which are managed on an average rotation time of 40–60 years (Petty, Garson & McIntosh 1995). The trees are clear-felled and the next crop is then planted within 6 months to 1 year. Relatively large clear-fell patches (5–100 ha) are created and are colonized mostly by grasses. These grassland patches persist until the young trees shade out the grasses (approximately 15 years after planting). The forest therefore consists of a mosaic of dense conifer stands with little ground vegetation and ephemeral grassland patches. Open moorland and agricultural land
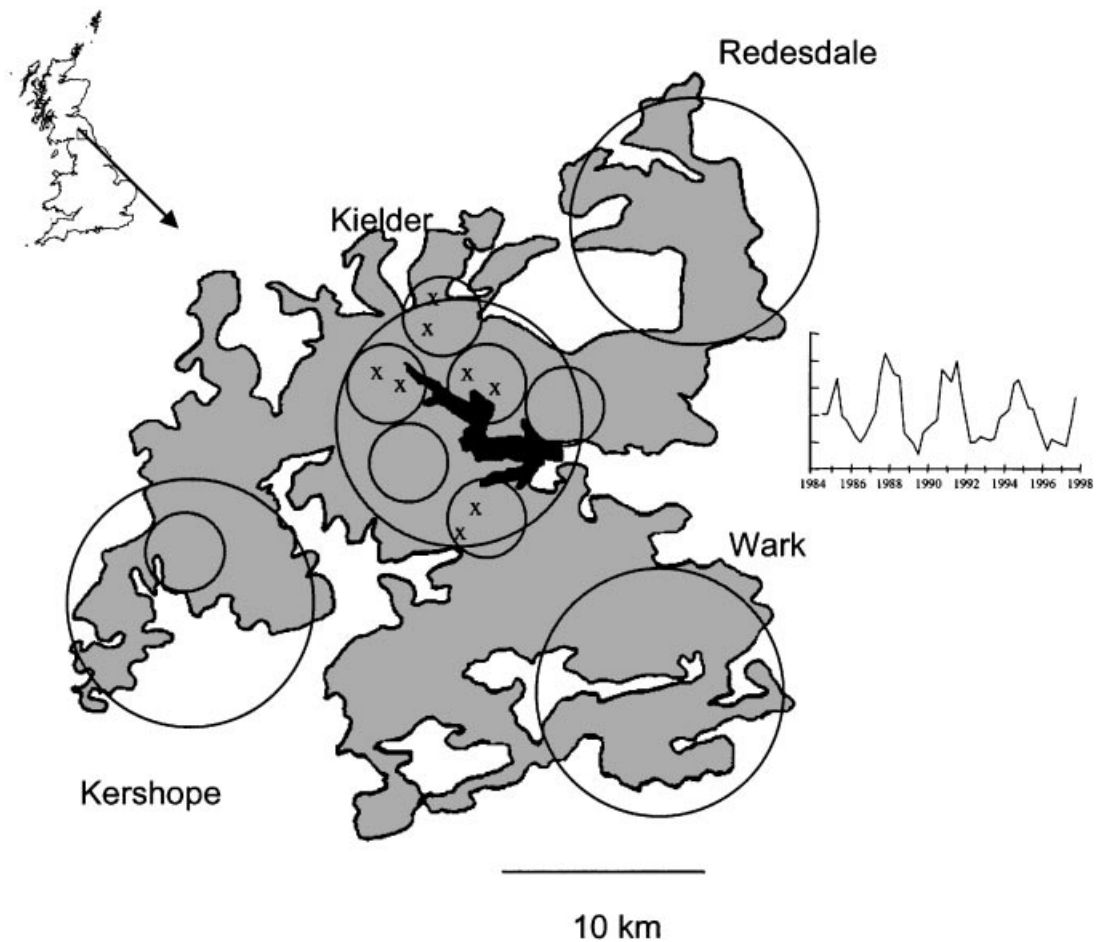
Fig. 1. Variation in vole densities was sampled at three spatial scales in the forested area (grey shading). Seven different sampling sites were located within each of the circles and each of the patches indicated by crosses. Densities were assessed in Kershope, Kielder, Wark and Redesdale forests, six valleys were sampled around Kielder reservoir (black shading) and a further valley was sampled in Kershope. The black crosses indicate the approximate positions of the separate grassland patches that were used as the smallest sampling scale. The insert indicates the changes in vole density in Kielder forest (after Lambin *et al*. 2000).

surround the forest and these are both poor habitats for field voles. Field voles live within the grassland areas but are not found in the dense spruce plantations (L. Thomson, unpublished data). Long-term monitoring has been restricted to Kielder watershed (Fig. 1), which is centred on a large reservoir within the plantation and has shown that field vole populations in Kielder have cyclic dynamics with a 3–4-year period as in much of Fennoscandia (Petty 1992; Lambin, Petty & MacKinnon 2000).

SAMPLING REGIME

Field vole abundance was assessed at 133 sampling sites from three spatial scales in both spring (March–April) and autumn (September–October) in 1996 and 1997 and in the spring of 1998. At the smallest scale, sampling was conducted within the same grassland patch (sites ranged from 0·1 to 0·8 km apart within areas of < 1 km^2). At the intermediate scale, sampling was conducted for sites in different patches but within the same valley (sites ranged from 0·9 to 5·1 km apart within areas of approximately 10 km^2). At the largest

scale, the sampling sites were in separate patches within watersheds separated from each other by moorland or agricultural land (sites ranged from 1·1 to 12·5 km apart within areas of approximately 70 km^2). Eight patches (mean size 9·3 ha, range 3·5–15·5 ha), seven valleys and four watersheds were sampled, and within each of those scales seven sampling sites were chosen to give an approximately even coverage of the area (Fig. 1). An additional 14 sites from across the forest were sampled for inclusion in spatial autocorrelation analyses. All sampling sites were located in grassland on surface water gley soils and the most common plant species were the grasses *Deschampsia cespitosa* Beauv., *Holcus lanatus* L., *Agrostis tenuis* Sibth. and a rush *Juncus effusus* L. At each site, 25 quadrats (25 × 25 cm) were searched for vole signs. Quadrats were placed by walking around the periphery of a 50 × 50 m area, and a square metal frame was thrown every 15–25 paces. If the metal quadrat fell on an area with no ground vegetation, it was thrown again. The number of quadrats that contained heaps of fresh (green) grass clippings was recorded as the vole sign index (VSI). This index has previously been calibrated against vole densities

calculated from capture–mark–recapture techniques (Lambin *et al.* 2000) and a separate calibration was used to convert the VSI scores to density in spring and autumn.

AUTOCORRELATION ANALYSIS

We described the scale over which logged vole densities (ln$D$, where D is density) were similar using Moran autocorrelations (Oden & Sokal 1986) for each of the five sampling sessions. Moran correlograms were constructed in which the significance of the Moran coefficient was assessed in each of 10 distance classes of equal range. Significant, positive Moran *I*-values indicated that sites within that distance class had densities that were more similar than average and the lowest value for the *x*-intercept was used as a measure of the domain over which densities were similar (Bjørnstad 1997).

Mantel correlations (Oden & Sokal 1986; Legendre & Fortin 1989; Fortin & Gurevitch 1993; Legendre 1993) based on cross-correlations were used to check for spatial patterns in the synchrony of changes in density (ln$D$). Anisotropy (directionality) in the pattern of synchrony was checked by calculating distances between sites after projection of the sites onto an axis passing through the centroid position of the sampling sites with direction of $\theta°$ from north (Fig. 2). Tests of anisotropy were performed for the whole data set and separately for each of the four watersheds. Significance of each Mantel correlation coefficient was assessed using randomization tests with 1000 permutations (Manly 1991). In each randomization, we calculated the Mantel correlation for each integer value of θ from 0 to 180° and stored the most negative value. One-tailed significance levels are based on the proportion of the stored values exceeding the observed correlation in magnitude. Hence, the test is for extreme, negative, Mantel correlations without conditioning on the associated direction. Moran autocorrelations were calculated using the R package, version 3·0 (Legendre & Vaudor 1991), and Mantel autocorrelations were implemented in Genstat 5 version 3·1. In all autocorrelation analyses, only one density estimate was used per grassland patch. In cases where the multiple estimates had been obtained within single patches, the estimates of density were averaged and the centre of the patch was used as the sampling location.

TRAVELLING WAVE ANALYSIS

A generalized additive model (GAM) was used to test for the presence of a travelling wave in the vole density data. A full description can be found in Lambin *et al.* (1998) and Elston *et al.* (in press). It demonstrated the presence of a travelling wave-like pattern when it was applied to a 13-year vole density time series (1984–97) which was collected from 21 sites within 5·5 km of Kielder reservoir (Lambin *et al.* 1998). The data set presented here covered a much wider geographical area and a 2·5-year period. The maximum likelihood estimates (MLE) of the direction and speed of the

travelling wave calculated from the model were compared with those estimated by Lambin *et al.* (1998).

We followed the method of Elston *et al.* (in press) using only one estimate per grassland patch ($n = 97$ sites). We fitted a model assuming that a travelling wave moved in one dimension towards a direction (θ–180) such that all sites experienced the same temporal change in density, but the density at any point in time was assumed to depend on the site's position along an axis of $\theta°$. Mathematically, the model was fitted as

$$\log D(i,t) = m + s[t + r (\cos\theta y_i + \sin\theta\, x_i)] + w(i) + e(i,t) \qquad \text{eqn 1}$$

where $D(i,t)$ is the estimated density at site *i* and time *t*, *m* is the overall mean, *s*(*t*) is a smoothing spline describing the temporal change in vole density, (θ) is the direction of the travelling wave, 1/*r* is the constant speed of the wave, y_i and x_i are, respectively, the distance north and east from the centroid and $e(i,t)$ are normally distributed residuals. The watershed factor *w*(*i*) was included to cater for the possibility that there may be consistent differences in density between different watersheds. There were too few observation times to investigate the degrees of freedom of the smoothing spline appropriate to characterize the cycle in the model that assumed no wave. Lambin *et al.* (1998) used the same model and showed that 21 degrees of freedom provided a parsimonious fit to a 13-years time series of vole data that covered four complete cycles in one of the four watersheds considered here. Five degrees of freedom were therefore used to fit the travelling wave model in this study, since approximately one cycle was documented in the 2·5-year data set. The MLEs for *r* and θ were calculated by iterative quadratic minimization of the residual mean squares of the GAM in the parameter space of *r*·cosθ and *r*·sinθ. At each iteration, combinations of *r*·cosθ and *r*·sinθ were selected and the deviance of the GAM was assessed. The values of *r*·cosθ and *r*·sinθ that were chosen formed the nine design points of a central composite design (Cochran & Cox 1957) centred on the current best parameter estimates and with major and minor ellipse axes of twice the length of the respective standard errors (Lambin *et al.* 1998). From these, 95% confidence regions for the speed and direction of the travelling wave could be calculated.

VARIATION IN DENSITIES AT DIFFERENT SCALES

The seven estimated densities from each sampled area at each scale and at each time were summarized by calculating their sample variance. These variances were analysed using a generalized linear model to investigate the variance-mean relationship at each of the three scales of sampling. The gamma distribution generalizes the chi-squared distributions of variances from data with Normal distributions, and so was used in the analysis with a log link function.
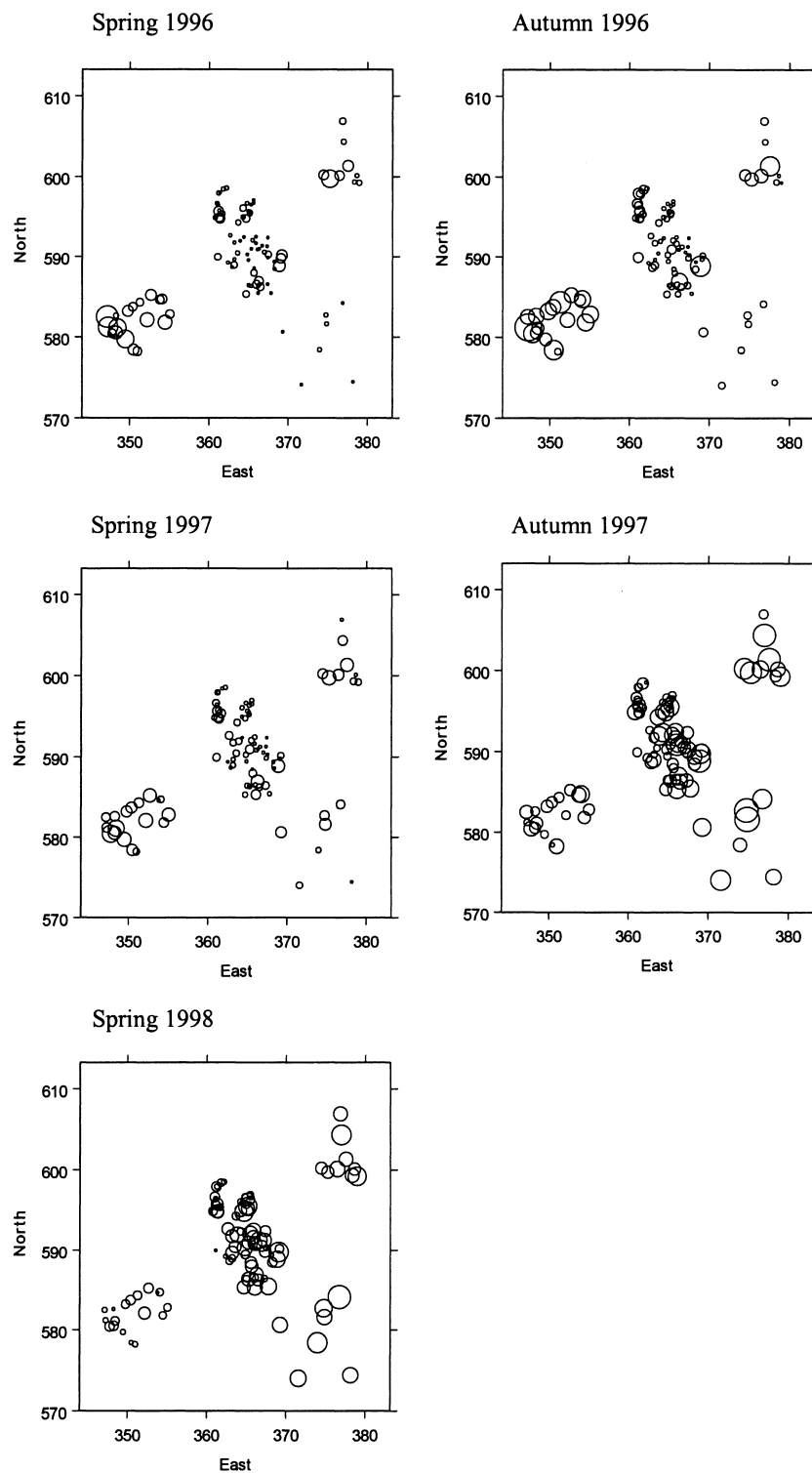
Fig. 2. The vole densities calculated at each sampling session. The centre of each circle represents the position of the sampling site and the diameter is proportional to the density recorded. Where more than one estimate was obtained for a single grassland patch, the average density is plotted. Units on both axes are in kilometres and the figures refer to the co-ordinates on Ordnance Survey British National Grid Square NY.

Results

Examination of the density data from 97 sites (Fig. 2) shows that vole densities were initially high in the south-west of the study area (Kershope watershed) in spring 1996 and peaked in autumn 1996 before declining.

In contrast, the other three watersheds had low densities in spring 1996 and subsequently increased.

The spatial autocorrelations showed that in all sampling sessions, the degree of similarity in vole density decreased with increasing distance between sampling sites (Fig. 3). The lowest *x*-intercepts of the Moran
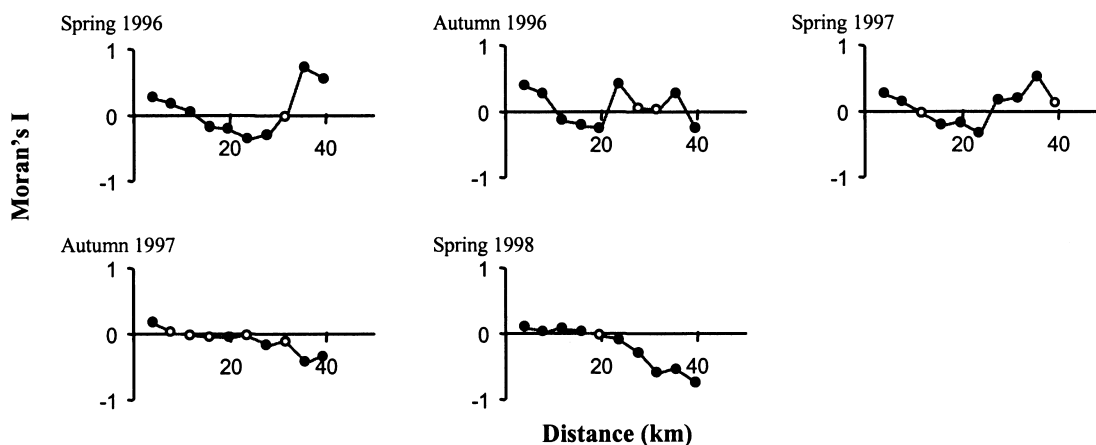
Fig. 3. Correlograms showing the Moran autocorrelation coefficients calculated from ln Density at each of 10 Euclidean distance classes with equal range. A separate correlogram is shown for each of the five sampling sessions. Solid circles represent Moran *I*-values significant at $\alpha = 0.05$.
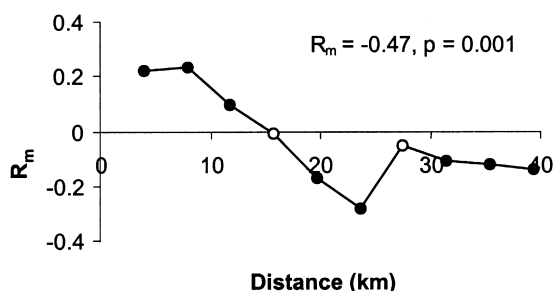

Fig. 4. Correlograms showing the Mantel correlation coefficient (R_m) based on cross-correlations of ln(Density) of each pairwise combination of sites and estimated for 10 equidistant distance classes. The significance of Mantel's R_m was assessed for each distance class using 1000 permutations of a randomization test. Solid circles represent significant autocorrelation values ($\alpha = 0.05$).

correlograms (estimated from Fig. 3) indicated an upper domain of similarity of vole density ranging from 8 to 20 (median = 11) km. In the first three sampling sessions the correlograms had a U shape, indicating that both close sites and distant sites (in the range of 25–40 km apart) had similar densities, consistent with expectation if a travelling wave swept through the area. In autumn 1997 and spring 1998 when vole densities were declining in the west of the study and increasing in the central and eastern watersheds, there was little spatial pattern in densities up to distances of 20 km. Densities were less similar than average beyond that distance. Thus, even though the pattern was consistent with a travelling wave in abundance, snap-shots in time did not always reveal a clear large-scale spatial pattern.

Mantel correlograms based on cross correlations of five density estimates indicated a significant decline of synchrony with distance (Fig. 4). The domain over which there was synchrony (positive cross-correlation values) was approximately 15 km but synchrony for sites 20–25 km apart was seemingly lower than for sites 30–40 km apart.

There was evidence of anisotropy in the spatial pattern of synchrony when the data from all four watersheds were included in the Mantel correlation calculations (Fig. 5). The Mantel correlation coefficient for the direction with the greatest spatial dependency (an axis of 72° from north) was higher ($R_m = -0.58$) than expected by chance if there was no anisotropy ($P < 0.001$). There was also evidence of anisotropy in the spatial pattern of synchrony when we considered the Kielder watersheds alone (an axis of 89° from north, $P < 0.01$) but no such evidence for the other watersheds for which fewer data were available.

We first fitted the travelling wave model to the data from all four watersheds. When we used a smoothing spline describing the temporal change in density without the travelling wave parameters, the residual sum of squares was 164·1 with 477 degrees of freedom. Ten iterations of the central composite algorithm were required to find the MLEs for r and θ. The residual sum of squares of the travelling wave model (equation 1) with the MLEs ($r = 0.0729$, $\theta = 246°$) was 141·7 with 475 degrees of freedom. This substantial improvement in the fit was gained by incorporating a travelling wave in the model moving in a direction 66° (95% confidence region: 47·7–132·3) to North with a speed of 14 km year^{-1}. The 95% confidence regions for the speed of the wave are contained within 10·6–19·4 km year^{-1}. The confidence region for estimates of the parameters $r \cdot \cos\theta$ and $r \cdot \sin\theta$ are shown in Fig. 6 with the equivalent plot for the 13 years time series. These show that the estimates of the speed and direction of the travelling wave in the two data sets were consistent (19 km year^{-1}, 95% confidence region: 11·2–40·0) along 78° (95% confidence region: 66–99·5°) for the 13 years data set. When the watershed factor was excluded from the GAM, the model yielded similar estimates for the speed and direction of the wave (22 km year^{-1} along an axis of 60°). These parameters did not differ significantly from either the model with the watershed included as a factor in the model, or from the model for
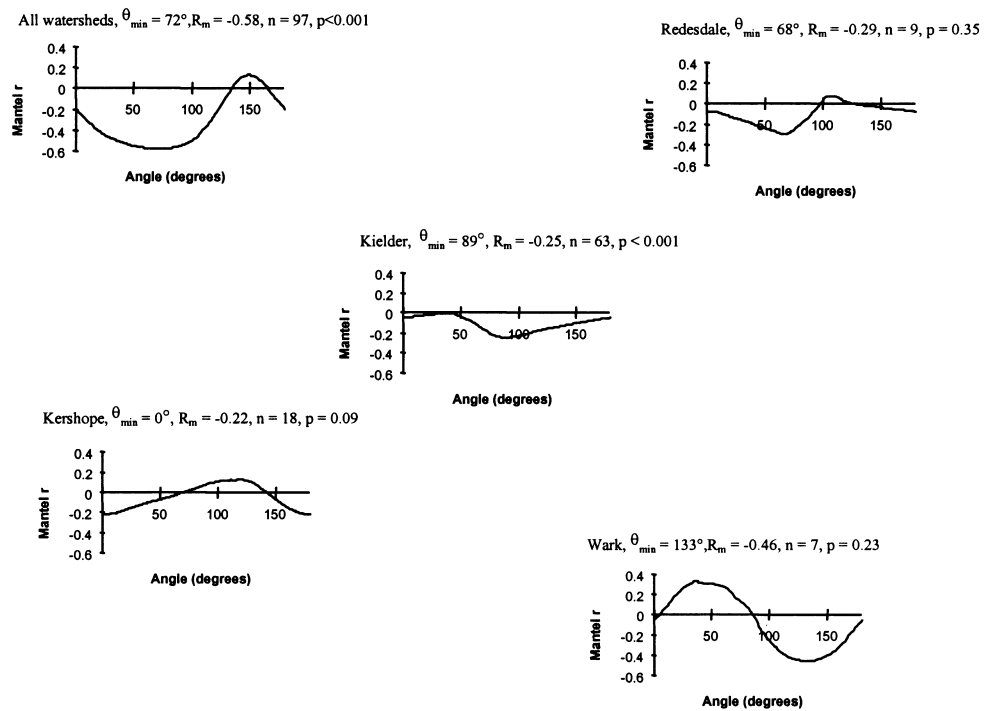
All watersheds, $\theta_{min} = 72°$, $R_m = -0.58$, n = 97, p<0.001

Redesdale, $\theta_{min} = 68°$, $R_m = -0.29$, n = 9, p = 0.35

Kielder, $\theta_{min} = 89°$, $R_m = -0.25$, n = 63, p < 0.001

Kershope, $\theta_{min} = 0°$, $R_m = -0.22$, n = 18, p = 0.09

Wark, $\theta_{min} = 133°$, $R_m = -0.46$, n = 7, p = 0.23

Fig. 5. The Mantel correlation coefficients calculated using distance classifications after projecting sampling sites onto an axis of $\theta°$ through the centroid of the study area. These tests of anisotropy in the pattern of synchrony were repeated for the complete data set and separately for each of the four watersheds. The values of $\theta°$ for which Mantel's *r* was most negative (θ_{min}), are indicated with significance values calculated using 1000 permutations of a randomization test and the number of sampling sites included in the analysis (*n*).
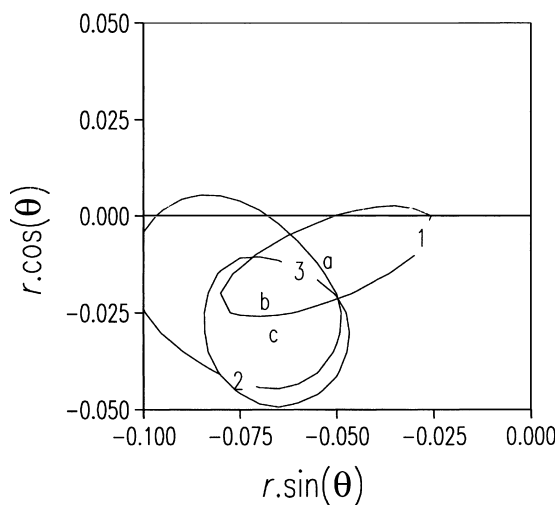

Fig. 6. The maximum likelihood estimates and 95% confidence regions of the parameters r.sinθ and r.cosθ from the generalized linear model used to detect travelling waves. Separate estimates and confidence regions are given for (a) the previously published 13 years data set (Lambin *et al*. 1998), (b) the new data set including all sampling sites, and (c) one random sample of the new data with only 15 sites included from Kielder (see text for details).

separate random samples and obtained estimates of the travelling wave parameters ranging from 12 to 15 km year^{-1} for speed and 63–78° for direction. We did not fit the GAMs separately to the data from each watershed as they covered only short segments of cycles (e.g. low and early increase phases in Kielder; peak and decline in Kershope). Thus, we found evidence consistent with a travelling wave moving along an axis from south-west to north-east at both the scale of the whole study area and within the Kielder watershed. There were no obvious geographical trends in the residuals from the GAM for each of the surveys or for the residuals summed over all sampling times, thus supporting the conjecture of one wave moving across the forest. There was also no evidence of larger residuals at the edges of the forest.

VARIATION IN DENSITIES AT DIFFERENT SCALES

The processes hypothesized to cause vole population synchrony vary in the scale at which they are likely to act and in their effect at different vole densities. We assessed the relationship between vole abundance and spatial variation in vole abundance at different scales by means of a generalized linear model to compare the variation (measured as the variance) in vole density estimates at different spatial scales. There was a positive relationship between variance and mean density, and so log(mean density) was included as a covariate in the model. The coefficient of log density in the fitted model

the 13-year time series. Most sampling sites (65%) were in Kielder where the travelling wave had previously been detected. We removed the bias in the number of sampling sites by including only 15 randomly chosen sites from Kielder. We repeated the analysis for 10

is an estimate of the power (b) of the mean to which the variance is related: variance = $\exp(a)*\text{mean}^b$. The best fitted model had different values of a for the different spatial scales ($a = 3{\cdot}01$ [SE = 0·68], 3·84 [SE = 0·70], 3·84 [SE = 0·74] for patch, valley and watershed scales, respectively, maximum SED = 0·22; $b = 0{\cdot}80$ [SE = 0·15]). There was no evidence for b varying with scale, nor for any effect of sampling session. Within patches, the variance–mean relationship was similar to that expected by binomial variance, and the dependence of a but not b on scale suggests that population synchrony was not affected by density at any of the sampling scales.

Discussion

In this study we sampled field vole populations at three spatial scales and used three different analytical methods to examine spatio-temporal patterns of vole density. Although this study covered a relatively short period, the data were consistent with the presence of a periodic travelling wave of vole densities occurring across the entire 600-km^2 forested landscape. When all the available data were examined, the estimated speed and direction of the wave were closely consistent with the previously published estimate based on data from a smaller geographical area (Lambin *et al*. 1998). The model assuming a travelling wave provided a significantly better fit to the data than models assuming no spatial pattern or different densities for each watershed. However, our results do not preclude the possibility that at smaller spatial scales the direction of the wave may vary, as we failed to detect significant directions within the Redesdale and Wark watersheds with the data available. Both methods used to study the relationship between variability in vole population densities and spatial scale, suggested that population densities were more similar at smaller sampling scales. The variation in densities was lowest within grassland patches, but the domain of synchrony was much larger than the average size of a grassland patch.

The pattern revealed differs from that revealed in other studies of fluctuating populations of rodents. In other studies, the spatial domain of synchrony is typically much larger within the range of 10–100 km (Steen, Ims & Sonerud 1996; Bjørnstad, Stenseth & Saitoh 1999a). The smaller domain of synchrony observed in our study must reflect the importance of factors other than climate and wide-ranging nomadic birds of prey (Petty *et al*. 2000) in regulating abundance in these populations. Both dispersal (Ranta *et al*. 1995a; Steen *et al*. 1996; Sherratt *et al*. 2000) and resident predators (Ydenberg 1987; Ims & Steen 1990; Korpimäki 1994; Bjørnstad *et al*. 1999b) are plausible processes for causing synchrony at scales of 10–100 km but separating their effects is difficult. The small domain of synchrony is explained by the presence of the travelling wave. An important question raised by this study is whether travelling waves are general properties of vole cycles. The graphical analysis of Giraudoux *et al*. (1997)

suggests that outbreaks of water vole (*Arvicola terrestris*) populations in France also occurred as a wave, spreading from epicentres over more than 2500 km^2 at a speed in excess of 10 km year^{-1}. Ranta & Kaitala (1997) presented some evidence for travelling waves in field vole populations in Finland, but Bjørnstad *et al*. (1999a) found no evidence for spatial patterns in a very thorough analysis of an exceptionally large data set on cyclic populations of the grey-sided vole (*Clethrionomys rufocanus* (Sund)) from Hokkaido. Certainly, the presence of waves in some cyclic vole populations does not support the recent contention by Bjørnstad (2000) that cyclicity should result in large-scale synchrony through the process of linear phase locking.

There was less variation in densities at the grassland patch scale than at either the valley or watershed sampling scales. Variation in density at all three scales was not related to mean vole density. These results indicate that a process that tends to 'equalise' population densities, which leads to population synchrony, is effective at the within-patch scale (at least for patches up to 15·5 ha). Dispersal of animals over short distances is the most plausible process to explain this result. The lack of relationship between variance in density and mean density suggests that the synchronizing process was not density-dependent during this study. However, it should be noted that most sites experienced an increase in density during this study and hence our results do not exclude the possibility that a density-dependent process could cause the travelling wave by causing the population decrease.

The Mantel tests for anisotropy on data for the whole region indicated that the spatial pattern of synchrony was strongest in the direction of 72° from north, which is identical to the direction recorded from the same analysis on data from a smaller spatial scale but longer temporal scale (Lambin *et al*. 1998). The shape of the Moran correlograms in the first three sampling sessions were also indicative of a regular spatial pattern in vole densities that was consistent with a wave (Legendre & Fortin 1989). Fitting the GAM indicated that the wave of densities moved in a direction of 66° with an approximate speed of 14 km year^{-1}. and that these values were consistent with Lambin *et al*.'s estimates. Hence, although the data were only collected over a 2·5-year period, and therefore does not include an entire cycle for any single sampling site, the model assuming a periodic travelling wave provided the best fit to the data because the spatial extent of the data set included four forests that were out of phase with each other (Fig. 2). Whereas this cannot be taken as a demonstration that the actual underlying pattern is a linear periodic travelling wave, the strength of evidence in favour of a spatial pattern resembling a travelling wave goes well beyond the somewhat simplistic analyses taken as evidence of travelling wave in vole abundance in France and Finland (Ranta & Kaitala 1997; Kaitala & Ranta 1998), and the graphical analyses for water voles in France (Giraudoux *et al*. 1997).

The axis remained in a roughly south-west to north-east direction when all the data were considered and when only 15 of the Kielder forest sites were included (to reduce sampling bias) and the confidence regions for the estimate of the direction and the speed of the assumed wave were wholly consistent with estimates derived from the historical data gathered over a much more restricted area. We interpret these analyses as indicating that there is a travelling wave of vole densities moving broadly along a south-west to north-east axis over the scale of the entire forested area, but there may be local modifications to the overall pattern. The absence of any pattern in the residual map, however, implies that the model is as good a fit throughout the forested area.

Little theory explicitly links the scale at which a process operates to the expected domain over which synchrony would subsequently be observed. Bjørnstad *et al.* (1999b) and Sherratt *et al.* 2000) noted that the scale at which a synchronizing diffusive process (such as dispersal) operates can be much smaller than the actual domain of synchrony. Similarly, having detected a travelling wave in vole densities, we are unable to link the pattern directly to the process causing it. Nevertheless, by sampling at multiple scales and using multiple analyses we are able to make some predictions about the process causing the wave. For travelling waves to occur, both a reaction process and a diffusive process must be involved (Kareiva 1990; Sherratt *et al.* 1997) and the diffusive process must lead to a movement of the wave in the order of 11–22 km year^{-1}. It is noteworthy that similar propagation speed are given by Giraudoux *et al.* (1997) for water voles in France. The direction of the wave probably gives little indication of the process responsible because models show that once a periodic travelling wave has been established, the direction does not change (Sherratt *et al.* 1997). Although dispersal by voles is unlikely to account for the periodic travelling wave pattern in itself, it may facilitate another process such as the spread of a disease between habitat patches. Hence, habitats that are dispersal barriers in the landscape may still modify the direction of the wave at a local scale. We did not have sufficient spatial resolution to test for this possibility, but it is noteworthy that the large-scale pattern seemed unaffected by the presence of moorland and unlogged forest on the high ground between the Kershope Kielder and Redesdale watersheds. Furthermore, Fig. 2 suggests that fluctuations in vole abundance in the Wark watershed were broadly synchronized with fluctuations in the Kielder watershed, consistent with a pattern at an even larger scale than that of the whole forested area.

Periodic travelling waves of vole densities are incompatible with the theoretical models of highly mobile predators causing synchrony of vole populations (De Roos, McCauley & Wilson 1991). Other models suggest that travelling waves are most likely to be caused by the effects of predators that have a limited mobility relative to their prey (Sherratt *et al.* 1997) or by the spread of a disease (Murray, Stanley & Brown 1986; Murray 1989).

Weasels (*Mustela nivalis* (L.)) are vole specialists that may play an important role in causing vole cycles (Hanski, Hansson & Henttonen 1991; Hanski *et al.* 1993; Korpimäki 1993; Hanski & Korpimäki 1995; Turchin & Hanski 1997) although at present this hypothesis has not been experimentally tested. The relatively small range size of weasels (Jedrzejewski, Jedrzejewska & Szymura 1995) and their potential for high reproductive rates (Jedrzejewska 1987; King 1989) and substantial impact on their prey makes them the most likely predatory candidate for causing periodic travelling waves.

There is some evidence of diseases initially invading host populations as a wave (Cully *et al.* 1997; Dwyer, Elkinton & Hajek 1998), but only anecdotal reports of the successive wave-fronts necessary for periodic travelling waves. Theoretical models of rabies spread predict that the host population behind the wave front can have cyclic or dampening cyclic dynamics (Anderson *et al.* 1981; Murray *et al.* 1986). In the case of microtines, there is presently no empirical or theoretical support for the hypothesis that pathogens may be responsible for the 3–5 years cycles of microtine rodents. There remains a need for more empirical data from natural populations to understand whether diseases can cause spatio-temporal patterns such as the periodic travelling waves we have documented in field vole densities.

Our approach of sampling from multiple spatial scales repeatedly over time has substantially increased our understanding of the spatio-temporal pattern of vole abundance in our study area. We have demonstrated that the pattern resembling a periodic travelling wave described by Lambin *et al.* (1998) is a phenomenon that occurs over an area of at least 600 km^2. Although we are unable to determine the cause of the travelling wave in vole densities we can exclude predation by wide-ranging predators and climatic factors as the causes of this spatio-temporal pattern. We hypothesize that predation by small vole specialists such as weasels or the recurrent spread of a disease are the most likely causes of the travelling waves. Further theoretical considerations that link the movement scale of the inhibitor (predator or disease) to the expected speed of the wave would be useful to further refine hypotheses about the cause of the waves.

References

Anderson, R.M., Jackson, H.C., May, R.M. & Smith, A.M. (1981) Population dynamics of fox rabies in Europe. *Nature*, **289**, 765–771.

Bjørnstad, O.N. (1997) *Statistical models for fluctuating populations: patterns and processes in time and space.* PhD Thesis, University of Oslo, Oslo.

Bjørnstad, O.N., Stenseth, N.C. & Saitoh, T. (1999a) The scale of population dynamics of voles and mice in northern Japan. *Ecology*, **80**, 622–637.

Bjørnstad, O.N., Ims, R.A. & Lambin, X. (1999b) Spatial population dynamics: analyzing patterns and processes of population synchrony. *TREE*, **14**, 427–432.

Cochran, W.G. & Cox, G.M. (1957) *Experimental Designs.* Wiley, New York.

Cruywagen, G.C., Kareiva, P. & Lewis, M.A. & Murray, J.D. (1996) Competition in a spatially heterogeneous environment – modelling the risk of spread of a genetically-engineered population. *Theoretical Population Biology*, **1**, 1–38.

Cully, J.F., Barnes, A.M., Quan, T.J. & Maupin, G. (1997) Dynamics of plague in a Gunnison's prairie dog colony complex from New Mexico. *Journal of Wildlife Diseases*, **33**, 706–719.

De Roos, A.M., McCauley, E. & Wilson, W.G. (1991) Mobility versus density-limited predator-prey dynamics on different spatial scales. *Proceedings of the Royal Society of London, Series B*, **246**, 117–122.

Dwyer, G. & Elkinton, J.S. & Hajek, A.E. (1998) Spatial scale and the spread of a fungal pathogen of gypsy moth. *American Naturalist*, **152**, 485–494.

Elston, D., Lambin, X. & Moss, R. (in press) Modelling space-phase relationships in cyclic populations. *Journal of Agricultural, Biological and Environmental Statistics.*

Fortin, M.-J. & Gurevitch, J. (1993) Mantel tests: spatial structure in field experiments. *Design and Analysis of Ecological Experiments* (eds S.M. Scheiner & J. Gurevitch). Chapman & Hall, New York.

Fredga, K., Fredriksson, R. & Bondrup-Nielsen, S. & Ims, R.A. (1993) Sex ratio, chromosomes and isozymes in natural populations of the wood lemming (*Myopus schisticolor*). *The Biology of Lemmings* (eds N.C. Stenseth & R.A. Ims), pp. 465–491. Academic Press, London.

Giraudoux, P., Delattre, P., Habert, M. & Quere, J.P., Deblay, S., Defaut, R., Duhamel, R., Moissenet, M.F., Salvi, D. & Truchetet, D. (1997) Population dynamics of fossorial water vole (*Arvicola terrestris* Scherman): a land use and landscape perspective. *Agriculture Ecosystems & Environment*, **66**, 47–60.

Grenfell, B.T., Wilson, K., Finkenstädt, B.F., Coulson, T.N., Murray, S., Albon, S.D., Pemberton, J.M., Clutton-Brock, T.H. & Crawley, M.J. (1998) Noise and determinism in synchronized sheep dynamics. *Nature*, **394**, 674–677.

Gurney, W.S.C., Veitch, A.R., Cruickshank, I. & McGeachin, G. (1998) Circles and spirals: population persistence in a spatially explicit predator–prey model. *Ecology*, **79**, 2516–2530.

Hanski, I. & Korpimäki, E. (1995) Microtine rodent dynamics in Northern Europe: parameterized models for the predator–prey interaction. *Ecology*, **76**, 840–850.

Hanski, I. & Hansson, L. & Henttonen, H. (1991) Specialist predators, generalist predators, and the microtine rodent cycle. *Journal of Animal Ecology*, **60**, 353–367.

Hanski, I., Turchin, P. & Korpimäki, E. & Henttonen, H. (1993) Population oscillations of boreal rodents: regulation by mustelid predators leads to chaos. *Nature*, **364**, 232–235.

Holmes, E.E., Lewis, M.A., Banks, J.E. & Veit, R.R. (1994) Partial differential equations in ecology: spatial interactions and population dynamics. *Ecology*, **75**, 17–29.

Ims, R.A. & Steen, H. (1990) Geographical synchrony in microtine population cycles: a theoretical evaluation of the role of nomadic avian predators. *Oikos*, **57**, 381–387.

Jedrzejewska, B. (1987) Reproduction of weasels *Mustela nivalis* in Poland. *Acta Theriologica*, **32**, 493–496.

Jedrzejewski, W. & Jedrzejewska, B. & Szymura, L. (1995) Weasel population response, home range, and predation on rodents in a deciduous forest in Poland. *Ecology*, **76**, 179–195.

Kaitala, V. & Ranta, E. (1998) Travelling wave dynamics and self-organization in a spatio-temporally structured population. *Ecology Letters*, **1**, 186–192.

Kareiva, P. (1990) Population dynamics in spatially complex environments: theory and data. *Philosophical Transcations of the Royal Society of London, Series B*, **330**, 175–190.

King, C.M. (1989) *The Natural History of Weasels and Stoats.* Christopher Helm, London.

Koenig, W.D. & Knops, J.M.H. (1998) Testing for spatial autocorrelation in ecological studies. *Ecography*, **21**, 423–429.

Korpimäki, E. (1993) Regulation of multiannual vole cycles by density-dependent avian and mammalian predation? *Oikos*, **66**, 359–363.

Korpimäki, E. (1994) Rapid or delayed tracking of multiannual vole cycles by avian predators? *Journal of Animal Ecology*, **63**, 619–628.

Lambin, X., Elston, D.A., Petty, S.J. & MacKinnon, J.L. (1998) Spatial asynchrony and periodic travelling wave in cyclic field vole populations. *Proceedings of the Royal Society of London, Series B*, **265**, 1491–1496.

Lambin, X., Petty, S.J. & MacKinnon, J.L. (2000) Cyclic dynamics in field vole populations and generalist predation. *Journal of Animal Ecology*, **69**, 106–118.

Legendre, P. & Fortin, M.-J. (1989) Spatial pattern and ecological analysis. *Vegetatio*, **80**, 107–138.

Legendre, P. & Vaudor, A. (1991) *The R Package: Multidimensional Analysis, Spatial Analysis.* Université de Montreal, Quebec.

Legendre, P. (1993) Spatial autocorrelation: trouble or new paradigm? *Ecology*, **74**, 1659–1673.

Lele, S. & Tapper, M.L. & Gage, S. (1998) A spatial analysis of population dynamics in space and time using estimating functions. *Ecology*, **79**, 1489–1502.

Manly, B.F.J. (1991) *Randomization and Monte Carlo Methods in Biology.* Chapman & Hall, London.

McCauley, E. & Wilson, W.G. & De Roos, A.M. (1996) Dynamics of age-structured predator–prey populations in space: asymmetrical effects of mobility in juvenile and adult predators. *Oikos*, **76**, 485–497.

Mischaikow, K. & Hutson V. (1993) Travelling waves for mutualist species. *Siam Journal on Mathematical Analysis*, **24**, 987–1008.

Moran, P.A.P. (1953) Statistical analysis of the Canadian lynx cycle, II. Synchronization and meterology. *Australian Journal of Zoology*, **1**, 291–298.

Murray, J.D., Stanley, E.A. & Brown, D.L. (1986) On the spatial spread of rabies among foxes. *Proceedings of the Royal Society of London, Series B*, **229**, 111–150.

Murray, J.D. (1989) *Mathematical Biology.* Springer Verlag, New York.

Myers, R.A., Mertz, G. & Bridson, J. (1997) Spatial scales of interannual recruitment variations of marine, andromous, and freshwater fish. *Canadian Journal of Fisheries and Aquatic Sciences*, **54**, 1400–1407.

Oden, N.L. & Sokal, R.R. (1986) Directional autocorrelation: an extension of spatial correlograms to two dimensions. *Systematic Zoology*, **35**, 608–617.

Paradis, E., Baillie, S.R., Sutherland, W.J. & Gregory, R.D. (1999) Dispersal and spatial scale affect synchrony in spatial population dynamics. *Ecology Letters*, **2**, 114–120.

Petty, S.J. (1992) *Ecology of the tawny owl* Strix aluco *in the spruce forests of Northumberland and Argyll.* PhD Thesis, Open University, Milton Keynes.

Petty, S.J., Garson, P.J. & McIntosh, R. (eds) (1995) *Kielder – the ecology of a man-made spruce forest*, Vol. 79.

Petty, S.J., Lambin, X., Sherratt, N.T., Thomas, C.J., Mackinnon, J.L., Coles, C.F., Davison, M. & Little, B. (2000) Spatial synchrony in field vole *Microtus agrestis* abundance in a coniferous forest in northern England: the role of vole-eating raptors. *Journal of Applied Ecology*, **37** (suppl. 1), 136–147.

Pollard, E. (1991) Synchrony of population fluctuations: the dominant influence of widespread factors on local butterfly populations. *Oikos*, **60**, 7–10.

Ranta, E. & Kaitala, V. (1997) Travelling waves in vole population dynamics. *Nature*, **390**, 456.

Ranta, E. & Kaitala, V. & Lindström, J. (1997) Dynamics of Canadian lynx populations in space and time. *Ecography*, **20**, 454–460.

Ranta, E., Kaitala, V. & Lindström, J. & Lindén, H. (1995a) Synchrony in population dynamics. *Proceedings of the Royal Society of London, Series B*, **62**, 113–118.

Ranta, E., Lindström, J. & Lindén, H. (1995b) Synchrony in tetraonid population dynamics. *Journal of Animal Ecology*, **64**, 767–776.

Royama, T. (1992) *Analytical Population Dynamics.* Chapman & Hall, London.

Sherratt, J.A., Eagan, B.T. & Lewis, M.A. (1997) Oscillations and chaos behind predator–prey invasion: mathematical artifact or ecological reality? *Philosophical Transactions of the Royal Society of London, Series B*, **352**, 21–38.

Sherratt, T.N., Lambin, X., Petty, S.J., MacKinnon, J.L., Coles, C.F. & Thomas, C.J. (2000) Use of coupled oscillator models to understand synchrony and travelling waves in populations of the field vole *Microtus agrestis* in northern England. *Journal of Applied Ecology*, **37** (Suppl. 1),148–158.

Smith, C.H. (1983) Spatial trends in Canadian snowshoe hare, *Lepus americanus*, population cycles. *Canadian Field-Naturalist*, **97**, 151–160.

Steen, H. & Ims, R.A. & Sonerud, G.A. (1996) Spatial and temporal patterns of small-rodent population dynamics at a regional scale. *Ecology*, **77**, 2365–2372.

Sutcliffe, O.L., Thomas, C.D. & Moss, D. (1996) Spatial synchrony and asynchrony in butterfly population dynamics. *Journal of Animal Ecology*, **65**, 85–95.

Turchin, P. & Hanski, I. & Hanski, I. (1997) An empirically based model for latitudinal gradient in vole population dynamics. *American Naturalist*, **149**, 842–874.

Underwood, A.J. & Chapman, M.G. (1996) Scales of spatial patterns of distribution of intertidal invertebrates. *Oecologia*, **107**, 212–224.

Wiens, J.A. (1989) Spatial scaling in ecology. *Functional Ecology*, **3**, 385–397.

Ydenberg, R.C. (1987) Nomadic predators and geographical synchrony in microtine population cycles. *Oikos*, **50**, 270–272.